Electronic Supplementary Material (ESI) for Journal of Materials Chemistry C.

Van der Waals Epitaxial Growth and High-Temperature Ferrimagnetism in Ultrathin Crystalline Magnetite (Fe_3O_4) Nanosheets†

Yunzhou Xue,‡*[a] Hongtao Liu,‡[b] Yi Zhang,[c] Shenghuang Lin,[d] Shu Ping Lau*[e]

[a] College of Chemistry and Environmental Engineering, Shenzhen University, Shenzhen 518052, P.R. China. Orcid.org/0000-0002-2908-9032. E-mail: xueyz@iccas.ac.cn

[b] Department of Physics, The Hong Kong University of Science and Technology, Clear Water Bay, Hong Kong, P.R. China. Orcid.org/0000-0003-0500-7204

[c] School of Physics, Sun Yat-Sen University, Guangzhou 510275, P.R. China

[d] Songshan Lake Materials Laboratory, Dongguan, Guangdong 523808, P.R. China

[e] Department of Applied Physics, The Hong Kong Polytechnic University, Hung Hom, Kowloon, Hong Kong, P.R. China. Orcid.org/0000-0002-5315-8472. E-mail: apsplau@polyu.edu.hk

‡ These authors contributed equally to this work.

Keywords:

van der Waals epitaxy, magnetite, anomalous Hall effect, Curie temperature, 2D magnet

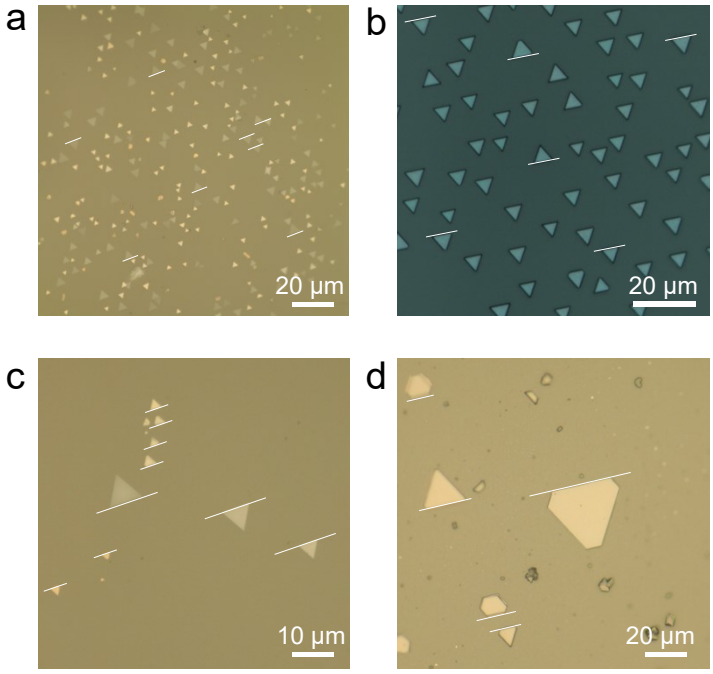

Figure S1. Optical images of Fe_3O_4 nanosheets grown on mica. (a,b) Ultrathin (a) and bulk-like (b) Fe_3O_4 nanosheets well aligned on mica. (c,d) Large size ultrathin (c) and bulk-like (d) Fe_3O_4 nanosheets on mica. White lines are the reference lines for calculation the orientation angle.

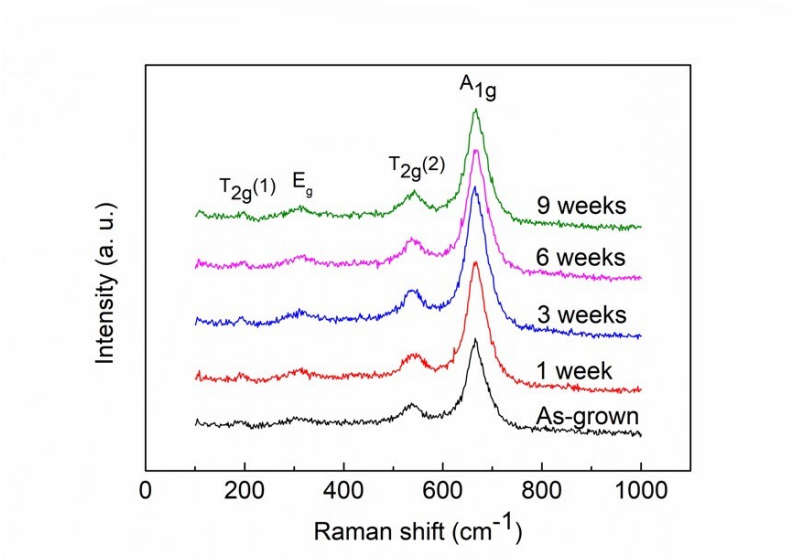

Figure S2. Raman spectra of the as-grown Fe_3O_4 nanosheets exposed in air for different times.

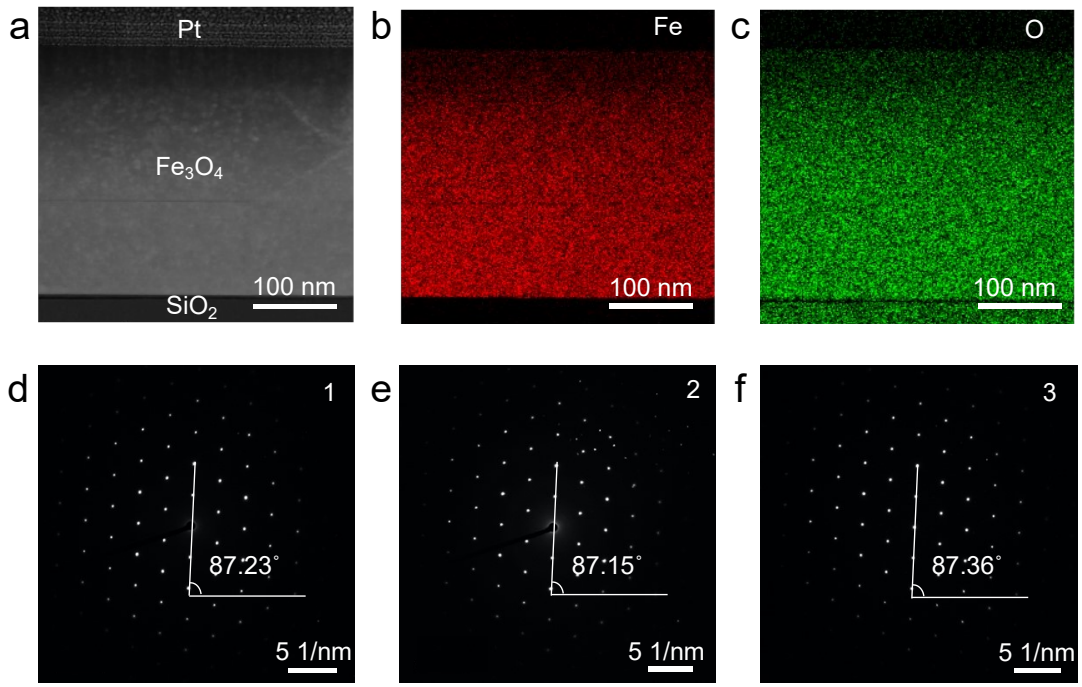

Figure S3. TEM image of cross-section of a Fe_3O_4 nanosheet. (a–c) Low-magnification TEM image (a) and its corresponding EDS mapping of Fe (b) and O (c). (d–f) SAED patterns were collected from the three corners marked with 1–3 in the inset in Figure 2a.

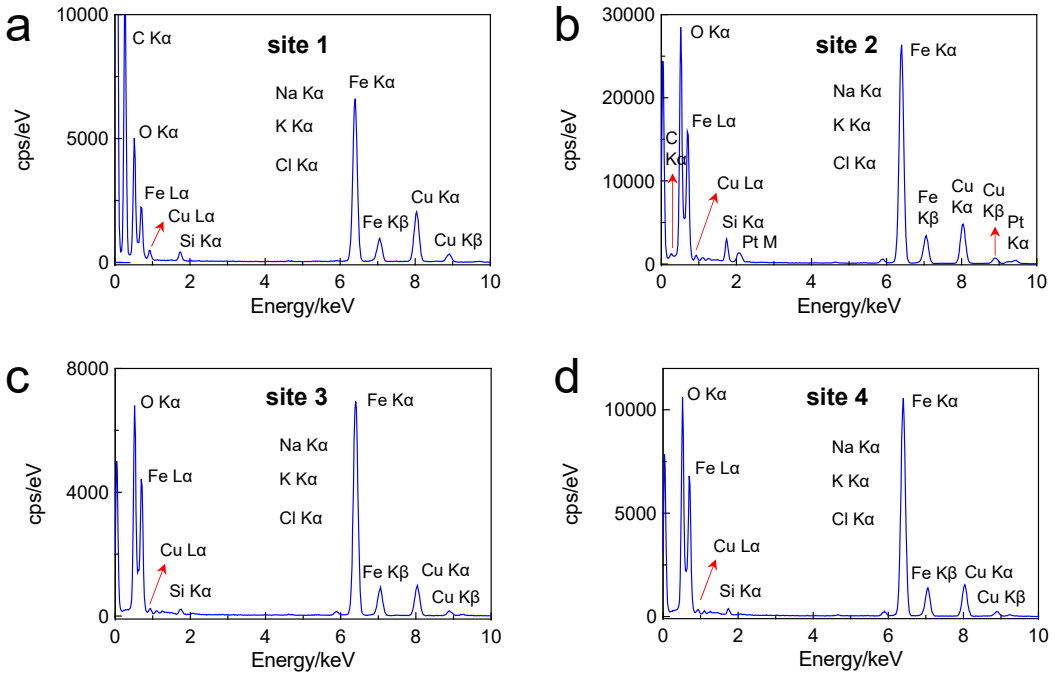

Figure S4. EDS spectra of the Fe_3O_4 nanosheets. (a) EDS spectrum of the top surface of a Fe_3O_4 nanosheet. (b–d) EDS spectrum of the cross-section of a Fe_3O_4 nanosheet. No salt contamination was observed in all the examined samples. Si signal may come from the mica substrate. Pt signal comes from the Pt thin film evaporated during the specimen preparation process, and subsequent FIB cut.

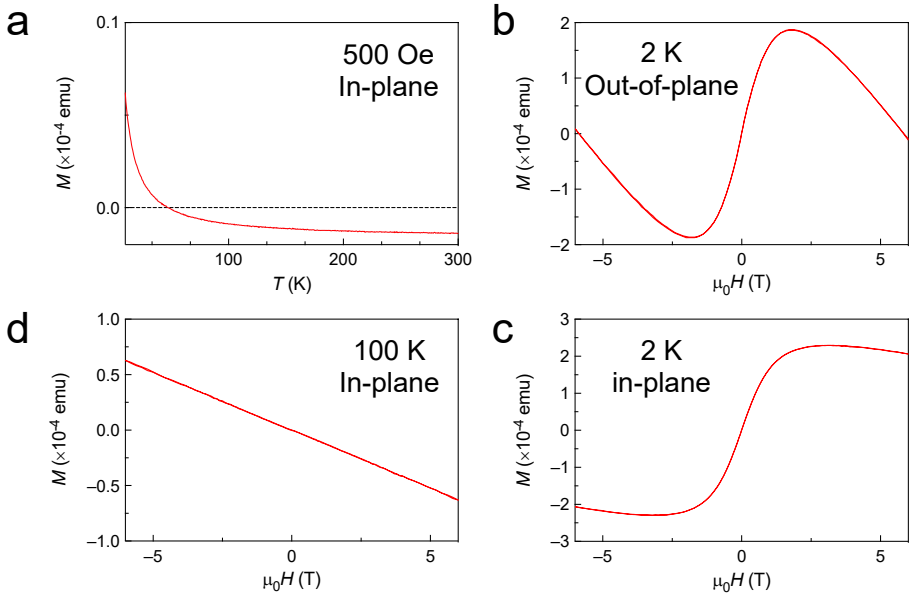

Figure S5. Magnetic properties of the mica substrate. (a) Temperature-dependent magnetization curve for the mica sheet. The applied magnetic field is 500 Oe and parallels the surface of the mica sheet. (b,c) Out-of-plane and in-plane magnetization curves at 2 K. (d) In-plane magnetization curves at 100 K.

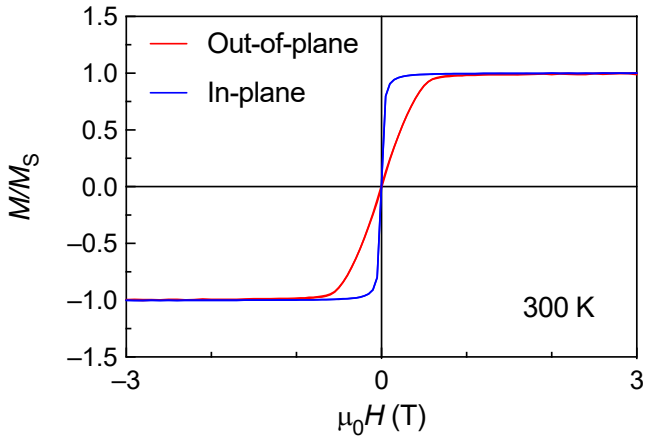

Figure S6. In-plane and out-of-plane magnetization curves of the Fe_3O_4 nanosheets at 300 K. In-plane and out-of-plane fields were applied parallel and perpendicular to the surface of the Fe_3O_4 nanosheets, respectively.

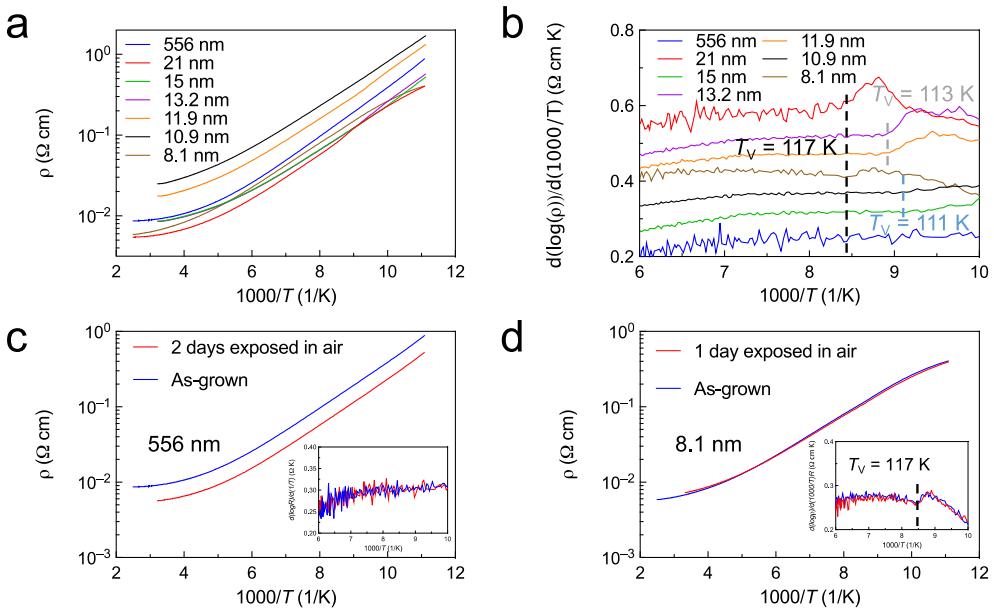

Figure S7. Temperature-dependent resistivity and the Verwey transition of the Fe_3O_4 nanosheets. (a) Temperature-dependent resistivity (ρ–T) of the different thickness Fe_3O_4 nanosheets. The linear parts in the curves can be fitted by the hopping transport model: $R(T) = R_0 exp(\frac{\Delta E}{k_B T})$. The active energy ΔE of the nanosheets are listed in Table S1. The Verwey transition can be seen at 117 K in the ρ–T curve of the 21 nm thick Fe_3O_4 nanosheet. (b) First derivative of the ρ–T curves in (a). The Verwey transition can be seen in all the Fe_3O_4 nanosheets except the 556 nm one. The onset transition temperature is marked by dash lines. (c,d) ρ–T curves of the as-grown and air-exposed 556 and 8.1 nm thick Fe_3O_4 nanosheets. The insets show the first derivative of the ρ–T curves.

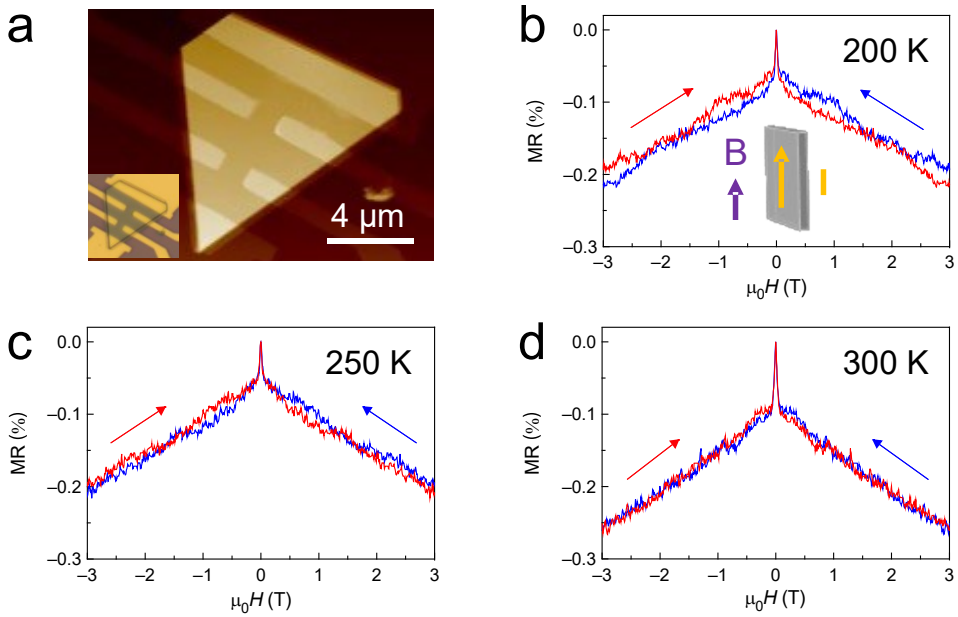

Figure S8. (a) AFM image of the Hall bar device based on the 556 nm thick Fe_3O_4 nanosheet. Its corresponding optical image is shown in the inset. (b–d) Longitudinal in-plane MR of the Fe_3O_4 nanosheet at different temperatures.

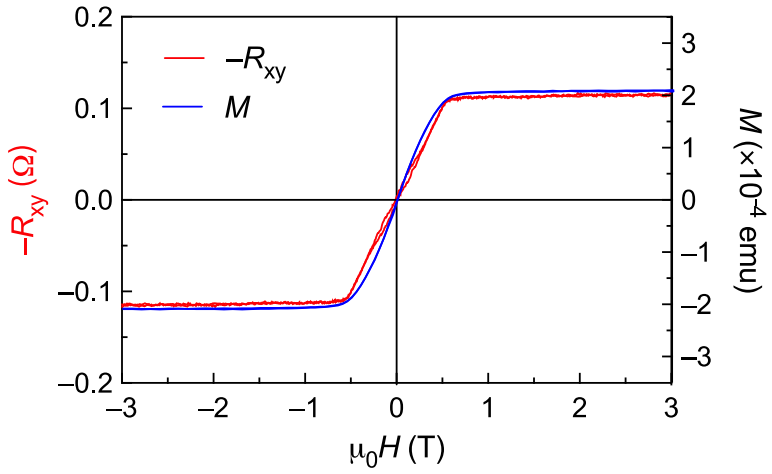

Figure S9. The relationship between the AHE (556 nm) and magnetization of the Fe_3O_4 nanosheets at 300 K in the out-of-plane field.

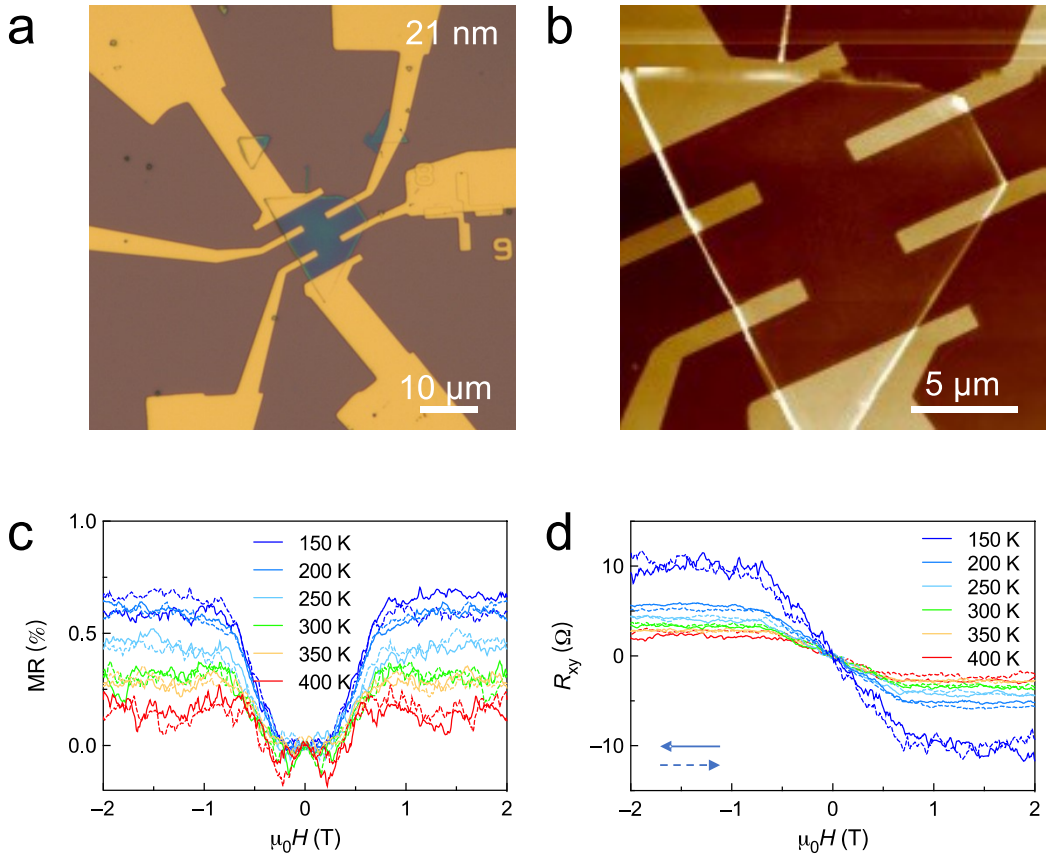

Figure S10. (a,b) Optical image (a) and its corresponding AFM image (b) of the Hall bar device based on the 21 nm thick Fe_3O_4 nanosheet. (c) Out-of-plane MR of the Fe_3O_4 nanosheet at different temperatures. (d) The AHE in the Fe_3O_4 nanosheet at different temperatures. The arrows represent the field sweep direction.

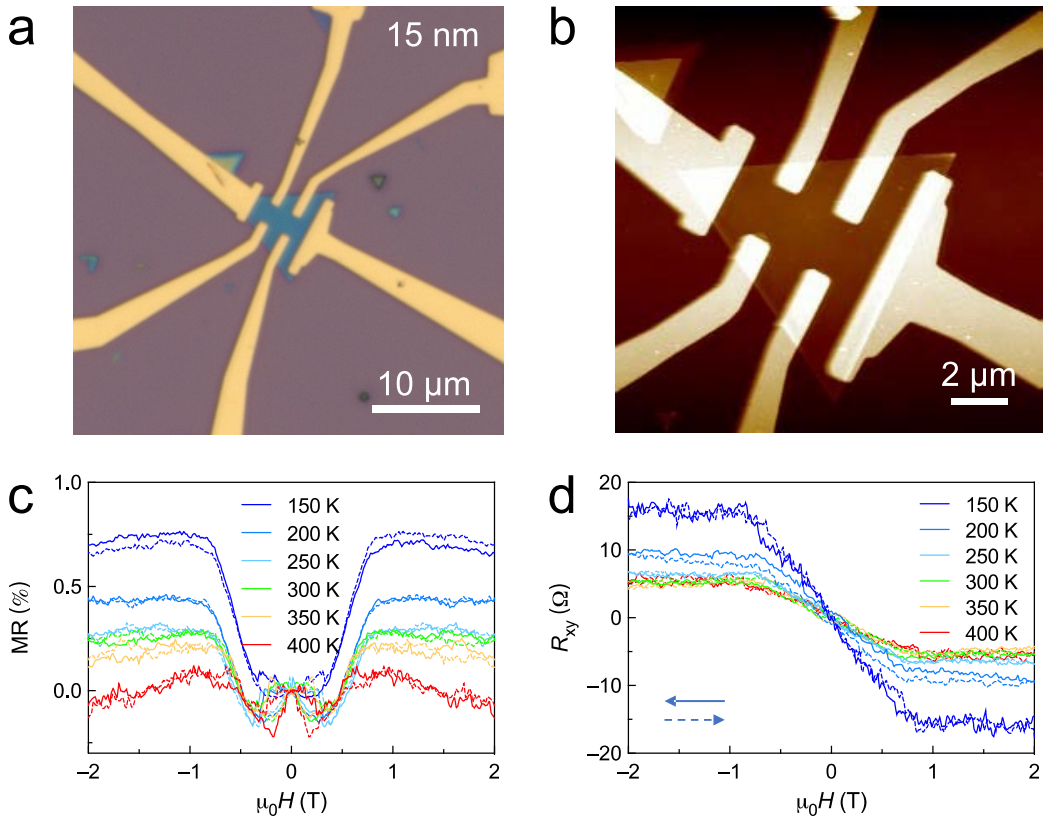

Figure S11. (a,b) Optical image (a) and its corresponding AFM image (b) of the Hall bar device based on the 15 nm thick Fe_3O_4 nanosheet. (c) Out-of-plane MR of the Fe_3O_4 nanosheet at different temperatures. (d) The AHE in the Fe_3O_4 nanosheet at different temperatures.

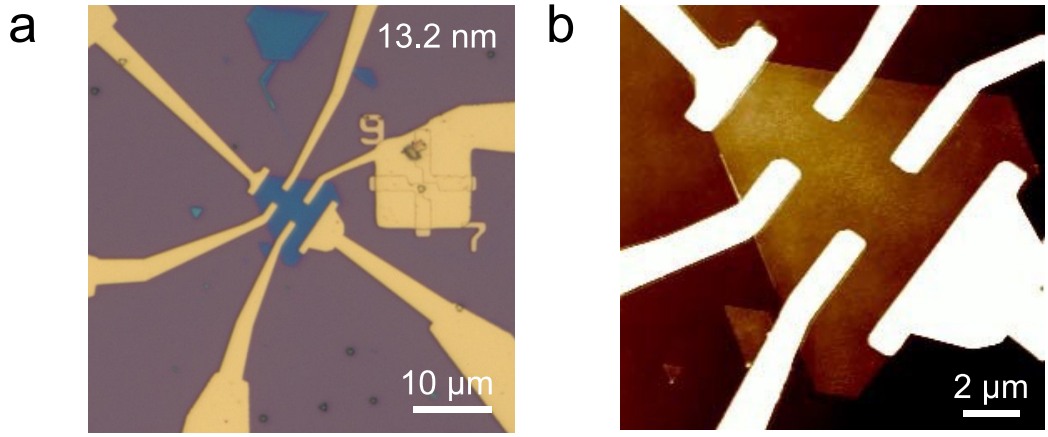

Figure S12. (a,b) Optical image (a) and its corresponding AFM image (b) of the Hall bar device based on the 13.2 nm thick Fe_3O_4 nanosheet.

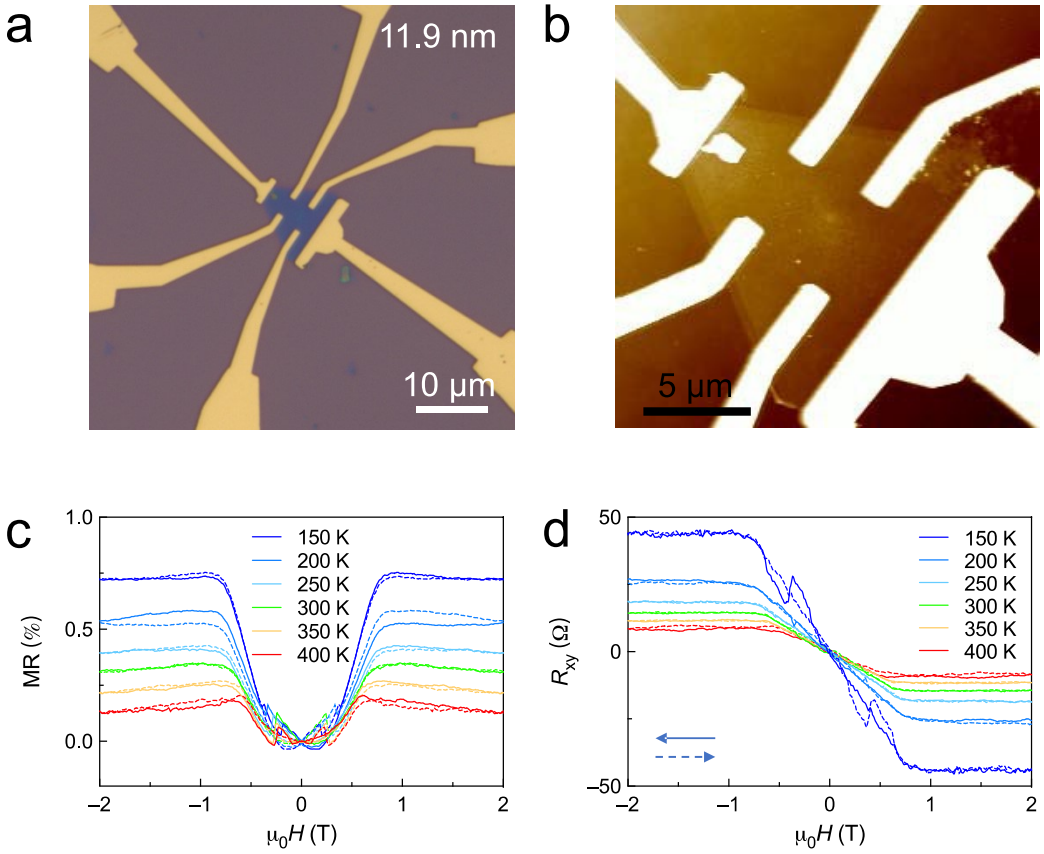

Figure S13. (a,b) Optical image (a) and its corresponding AFM image (b) of the Hall bar device based on the 11.9 nm thick Fe_3O_4 nanosheet. (c) Out-of-plane MR of the Fe_3O_4 nanosheet at different temperatures. (d) The AHE in the Fe_3O_4 nanosheet at different temperatures.

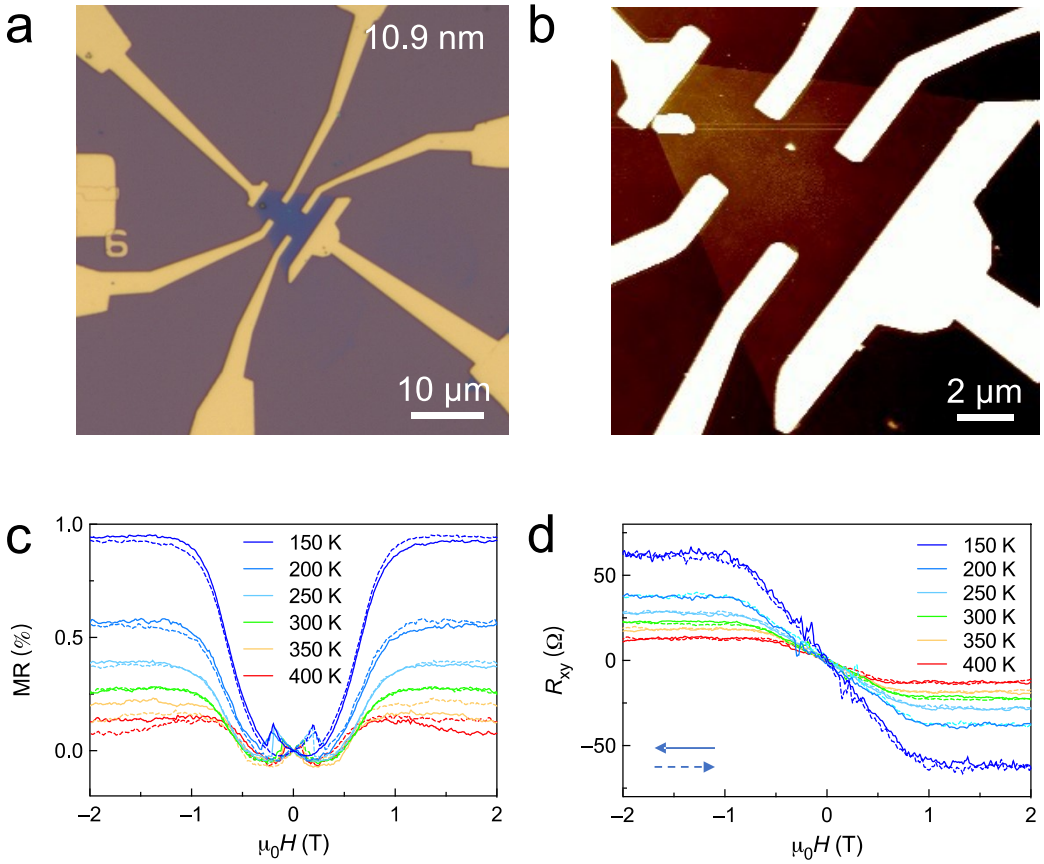

Figure S14. (a,b) Optical image (a) and its corresponding AFM image (b) of the Hall bar device based on the 10.9 nm thick Fe_3O_4 nanosheet. (c) Out-of-plane MR of the Fe_3O_4 nanosheet at different temperatures. (d) The AHE in the Fe_3O_4 nanosheet at different temperatures.

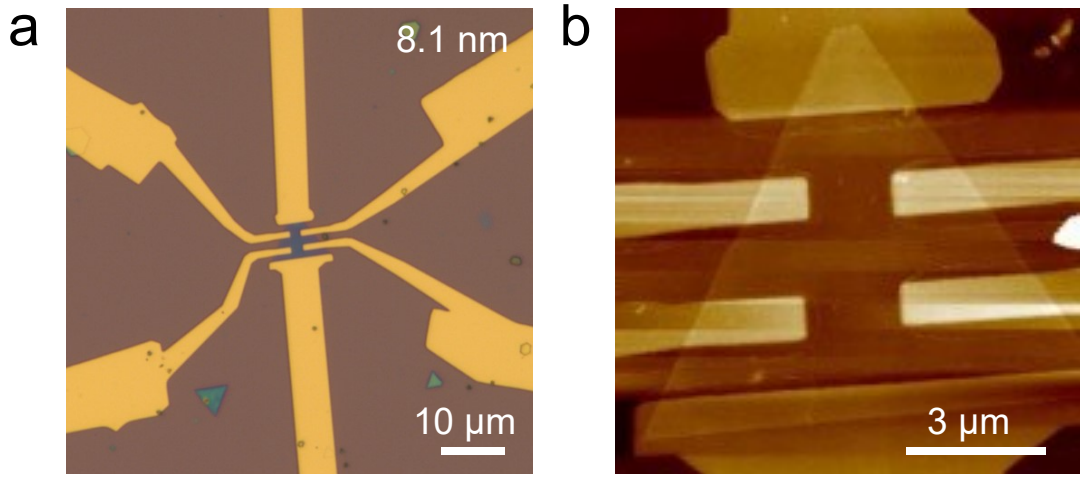

Figure S15. (a,b) Optical image (a) and its corresponding AFM image (b) of the Hall bar device based on the 8.1 nm thick Fe_3O_4 nanosheet.

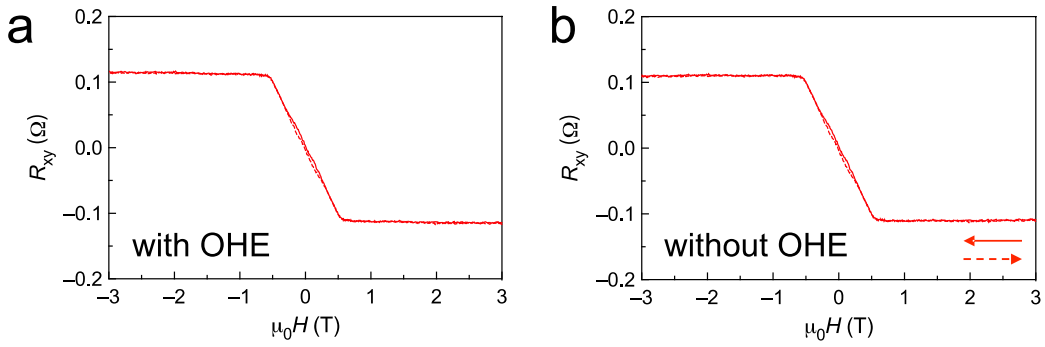

Figure S16. The anomalous Hall effect (556 nm, 300 K) with (a) and without (b) ordinary Hall effect (OHE).

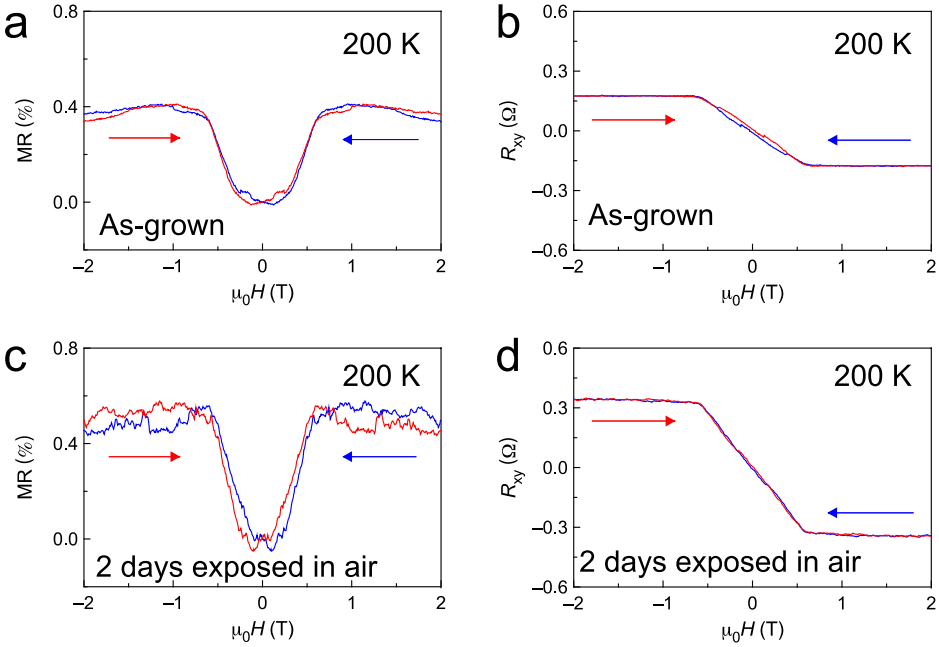

Figure S17. (a,b) Out-of-plane MR and the AHE in the as-grown 556 nm thick Fe_3O_4 nanosheet at 200 K. (c,d) Out-of-plane MR and the AHE in the Fe_3O_4 nanosheet at 200 K after 2 days exposing in air.

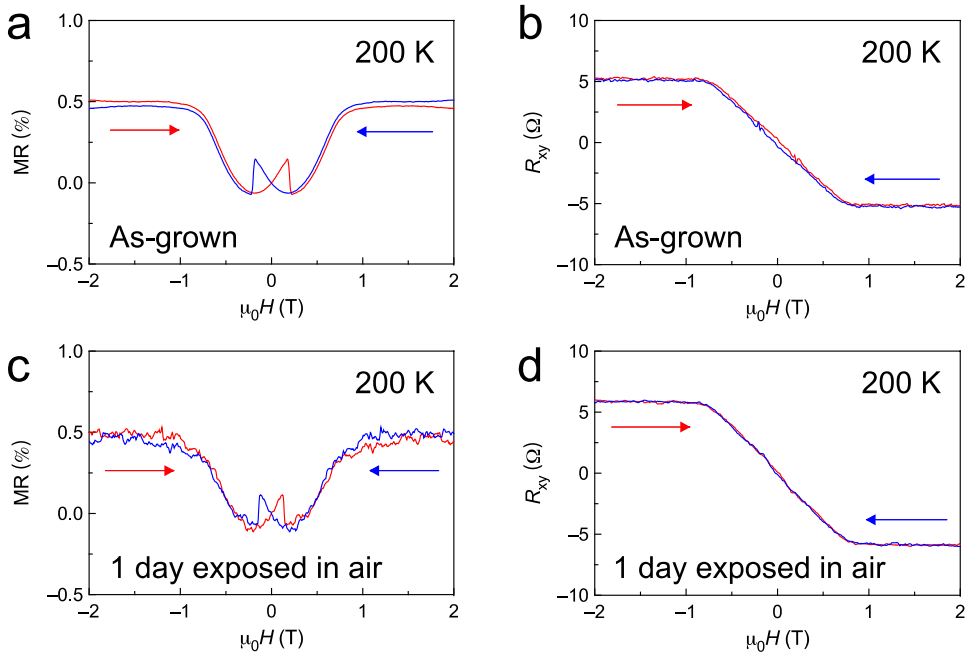

Figure S18. (a,b) Out-of-plane MR and the AHE in the as-grown 8.1 nm thick Fe_3O_4 nanosheet at 200 K. (c,d) Out-of-plane MR and the AHE in the Fe_3O_4 nanosheet at 200 K after 1 day exposing in air.

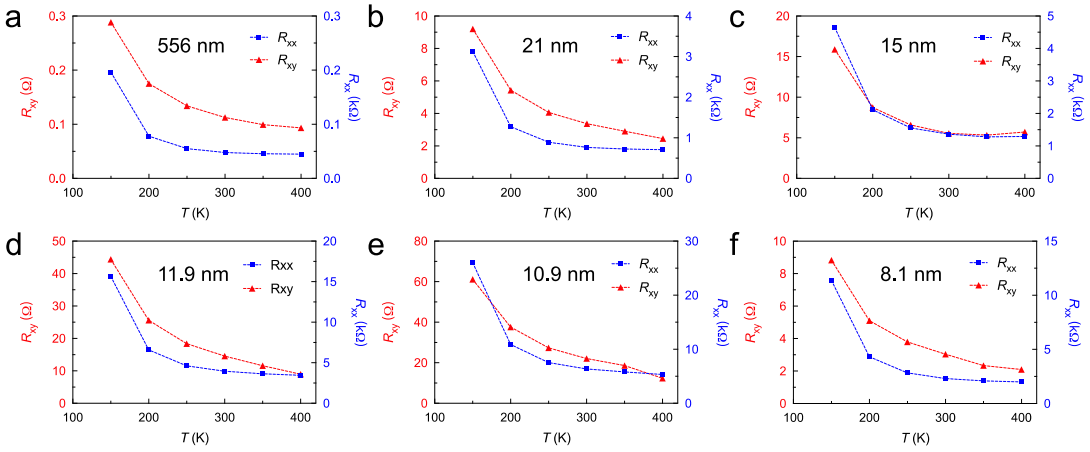

Figure S19. The temperature-dependent anomalous Hall resistance and longitudinal resistance of the Fe_3O_4 nanosheets with various thicknesses.

Table S1. Summary of parameters of all the devices measured

No.	**1**	**2**	**3**	**4**	**5**	**6**	**7**
Thickness/nm	556	21	15	13.2	11.9	10.9	8.1
ρ_{xx}/mΩ cm (rt)	9.3	5.9	8.7	8.6	17.6	25.1	6.8
T_V/K	—	117	110	113	113	111	117
E_a/meV	58.4	54.2	51.5	51.7	52.9	52	54.4
R_{xx}/kΩ (RT)	0.05	0.77	1.37	1.79	3.97	6.36	2.31
R_{xy}/Ω (RT)	0.11	3.37	5.56	6.04	14.54	22.12	3.04
ρ_{xy}/μΩ cm (RT)	5.53	6.07	8	6.6	13.8	20.2	1.89
Hall angle (%)	0.067	0.121	0.096	0.093	0.098	0.096	0.036

ρ_{xx} and R_{xx} stand for the longitudinal resistivity and longitudinal resistance, respectively;

ρ_{xx} and R_{xx} stand for the Hall resistivity and Hall resistance, respectively;

RT stands for room temperature, 300 K;

T_V stands for the Verwey transition temperature.